Available online at www.sciencedirect.com
ScienceDirect
Inorganica Chimica Acta 361 (2008) 1157–1165
Inorganica Chimica Acta
www.elsevier.com/locate/ica

X-ray photochemistry in iron complexes from Fe(0) to Fe(IV) – Can a bug become a feature?

Simon J. George [a], Juxia Fu [b], Yisong Guo [b], Owen B. Drury [c], Stephan Friedrich [a,c], Thomas Rauchfuss [d], Phillip I. Volkers [d], Jonas C. Peters [e,1], Valerie Scott [e], Steven D. Brown [e], Christine M. Thomas [e], Stephen P. Cramer [a,b,*]

[a] *Advanced Biological and Environmental X-ray Facility, Physical Biosciences Division, Lawrence Berkeley National Laboratory, Berkeley, CA 94720, United States*
[b] *Department of Applied Science, University of California, Davis, CA 95616, United States*
[c] *Advanced Detector Group, Lawrence Livermore National Laboratory, Livermore, CA 94550, United States*
[d] *Department of Chemistry, University of Illinois, Urbana, IL 61801, United States*
[e] *Division of Chemistry and Chemical Engineering, California Institute of Technology, Pasadena, CA 91125, United States*

Received 19 October 2007; accepted 28 October 2007
Available online 4 November 2007

Dedicated to Edward Solomon.

Abstract

Under intense soft X-ray irradiation, we have observed time-dependent changes in the soft X-ray spectra of virtually all the Fe coordination complexes that we have examined, indicating chemical transformation of the compound under study. Each compound, with oxidation states ranging from Fe(IV) to Fe(0), has been studied with either Fe L-edge spectroscopy or N K-edge spectroscopy. We find that very often a well-defined spectroscopic change occurs, at least initially, which is apparently capable of straightforward interpretation in terms of X-ray induced photoreduction, photooxidation or ligand photolysis. We briefly discuss the probable chemical nature of the changes and then estimate the rate of chemical change, thereby establishing the necessary radiation dose. We also demonstrate that the photochemistry not only depends on the Fe oxidation state but also the coordination chemistry of the complex. It seems that a proper understanding of such X-ray photochemical effects could well greatly assist the assignment of soft X-ray spectra of uncharacterized metal sites.

Keywords: Soft X-ray spectroscopy; Iron L-edge spectroscopy; Nitrogen K-edge spectroscopy; X-ray absorption spectroscopy; Metalloprotein; Radiation damage; X-ray photochemistry; Photoreduction; Photooxidation; Photolysis

1. Introduction

The issue of X-ray induced photochemistry arose almost immediately after the first X-ray absorption experiments on bioinorganic samples with synchrotron radiation. Powers and coworkers claimed that Cu(I)-like features in the Cu edge of cytochrome oxidase were the result of X-ray photoreduction [1]. Although this particular claim was later refuted (or at least disputed) [2], the flux densities

Abbreviations: pdt, propanedithiolate; $PhBP^{tBu}_2(pz')$, $[PhB(CH_2PtBu_2)_2(pz)]$ *(pz = pyrazolyl); PhBP*$_3$, *[PhB(*CH_2PPh_2*)*$_3$*]; dppv, cis*-1,2-bis(diphenylphosphino)ethylene; THF, tetrahydrofuran.

* Corresponding author. Address: Advanced Biological and Environmental X-ray Facility, Physical Biosciences Division, Lawrence Berkeley National Laboratory, Berkeley, CA 94720, United States. Tel.: +1 530 752 0360; fax: +1 530 752 2444.
E-mail address: spjcramer@ucdavis.edu (S.P. Cramer).
[1] Present address: Department of Chemistry, Massachusetts Institute of Technology, Cambridge, MA 02139, United States.

0020-1693/$ - see front matter © 2007 Elsevier B.V. All rights reserved.
doi:10.1016/j.ica.2007.10.039

available at that time were rather modest, $\sim 3 \times 10^9$ photons/s in a $0.4 \times 0.7\ mm^2$ spot. Subsequently, with $\sim 6 \times 10^{11}$ photons/s in a $2 \times 4\ mm^2$ spot, Chance and coworkers used EPR and on-line UV–Vis monitoring to demonstrate room temperature photoreduction of both Cu and heme components with $t_{1/2} < 5$ min [3]. Since then, fluxes have risen to as high as 10^{13} photons/s, while spot sizes range from a few mm^2 to as small as $0.1 \times 0.1\ mm^2$. Synchrotron radiation chemistry has been reported for a wide variety of metalloprotein samples, including Mn in photosystem II [4], Fe in superoxide reductase [5], a Rieske Fe–S cluster [6], the R2 protein of ribonucleotide reductase [7], heme proteins [8], and the nitrogenase FeMo-cofactor [9], Co in the B_{12} cofactor [10], Ni in superoxide dismutase [11,12], and Cu in stellacyanin [13], plastocyanin [14], and superoxide dismutase [15]. With almost 10^5 higher flux densities, radiation chemistry has gone from a theoretical possibility to an ever-present concern.

Of course, the issue of radiation damage is not unique to X-ray spectroscopy – the same concerns have been voiced for all experiments involving ionizing radiation, including protein X-ray diffraction [16,17], X-ray microscopy [18], electron diffraction [17,19] and electron microscopy [19]. Crystallographers are already up to their Fourth International Workshop on X-ray Damage to Biological Crystalline Samples [20]. Quantitative models for radiation damage, such as Henderson's limit [17], have been developed while numerous theoretical studies have addressed the relationships between microscope resolution, X-ray dose, and sample damage [18,21].

The issue of radiation chemistry is particularly important for measurement of biological samples using the soft X-ray range from 200 eV to 1000 eV. Measurements in this region are valuable to the bioinorganic chemist as it not only contains the light element K-edges with their $1s \rightarrow 2p$ transitions, but it also includes transition metal $L_{2,3}$-edges which are dominated by chemically sensitive $2p \rightarrow 3d$ transitions. Although the photon energies are about an order of magnitude lower than K-edges, the path lengths are about three orders of magnitude shorter, so that, for a given photon flux density, the energy deposited per unit volume is some 100-fold greater.

For a typical 'dilute' sample of 100 ppm Fe in an oxygen matrix, the ratio of metal to matrix cross section is 0.166×10^{-3} at the Fe L-edge (707 eV), compared to 2.55×10^{-3} at the Fe K-edge (7.112 keV). Moreover, the Fe $L_{2,3}$ fluorescence yield is 0.0128 compared with 0.34 for the K-edge [22]. Hence soft X-ray experiments take more time compared to the equivalent hard X-ray measurements, making the overall radiation dose greater. It is not surprising, therefore, that radiation chemistry often becomes the limiting factor for a successful soft X-ray experiment.

Referring to X-ray photochemistry as 'radiation damage' can be misleading, as this phrase implies non-specific chemical degradation of the sample. Many of the studies reporting metal photoreduction and site-specific chemical change suggest that well-defined X-ray photochemistry occurs, at least during the initial X-ray exposure. This leads to the prospect that measurement and interpretation of the X-ray photochemical properties of a sample could assist in spectral interpretation. In X-ray crystallography, it has been proposed to use the photochemical changes at specific sites as a phasing tool [23], a technique rather appropriately called "radiation-induced phasing" (RIP). These processes include the 'ablation' of carboxylate side chains, reduction of disulfides, and destruction of heavy atom centers [23]. For soft X-ray absorption spectroscopy, it implies that time-dependent spectroscopic and kinetic studies as a function of incident radiation intensity cannot only help in interpreting spectra, but also help establish the chemical identity of unknown species, such as a novel metal center in a metalloprotein.

In this paper, we examine time-dependent soft X-ray absorption spectra for a series of Fe complexes with formal oxidation states from Fe(0) to Fe(IV) (Scheme 1). In almost every case, we see changes in the spectra over time, indicating chemical transformation of the compound under study. We discuss the probable chemical nature of the observed changes and then estimate the rate of chemical transformation and the necessary radiation dose. Finally, we examine whether measurements of soft X-ray photochemistry could be a chemically useful tool.

2. Experimental

2.1. Sample preparation

Samples of $Fe^{I}_2(pdt)(PMe_3)(CN)(CO)_4$ [24], $(NEt_4)_2Fe^0(CO)_3(CN)_2$ [25], $[PhBP^{tBu}_2(pz')]Fe{\equiv}N(NtBu)^+$ [26], $[PhBP_3]Fe^{III}{\equiv}N(p\text{-tolyl})$ [27], and $[PhBP_3]Fe^{II}{\equiv}N(p\text{-tolyl})^-$ [27] were prepared as described elsewhere. $Fe^{II}(S_2C_2H_4)(CO)_2(PMe_3)_2$ was prepared by stepwise reactions of $FeCl_2$ with PMe_3, CO and $Na_2S_2C_2H_4$ in THF as detailed in the Supplementary material. $Fe^{II}(S_2C_2H_4)(CO)_2$(dppv) was similarly prepared but with *cis*-1,2-bis(diphenylphosphino)ethylene (dppv) instead of PMe_3, again as detailed in the Supplementary material. Other materials, including potassium ferricyanide, potassium ferrocyanide, ferric oxide, and boron nitride were obtained from Sigma–Aldrich. Samples for X-ray absorption spectroscopy (XAS) were prepared in a high integrity anaerobic (<0.5 ppm O_2) and dry glove box (Vacuum Atmospheres). Typically, finely ground powders were spread on double-sided carbon tape and sealed in the custom anaerobic sample holders [28]. These were subsequently transferred to the XAS vacuum chamber via a load-lock where the cap was removed. Special care was taken with the Fe(IV)-imide complex as this thermally decomposes at room temperature. In this case the sealed sample holders were immediately cooled in liquid nitrogen after preparation and mounted directly on pre-cooled cryostat cold fingers in both the load-lock and main sample chambers.

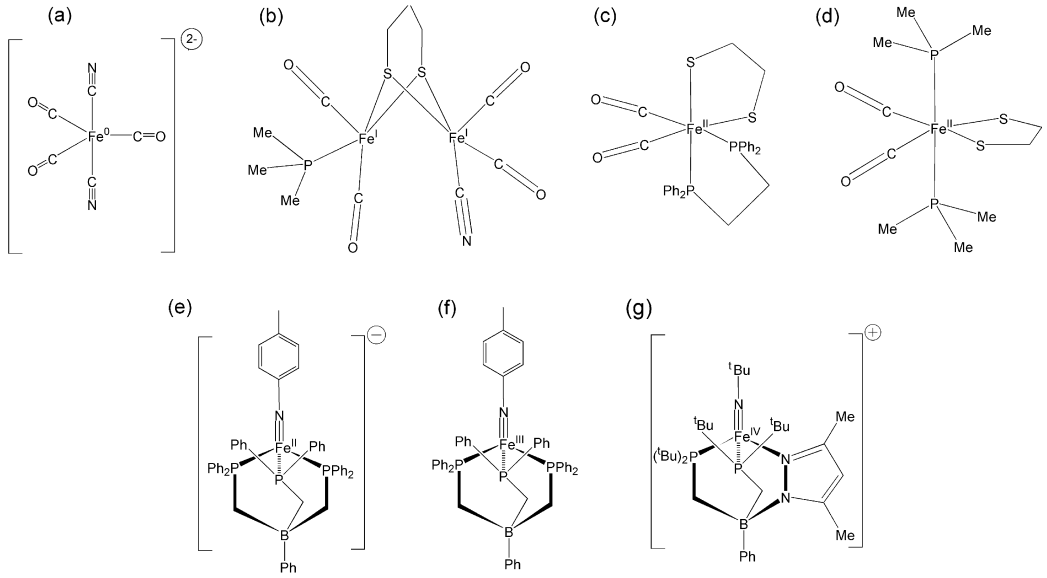

Scheme 1. Structures of complexes used in this study: (a) $(NEt_4)_2Fe^0(CO)_3(CN)_2$, (b) $Fe^I_2(pdt)(PMe_3)(CN)(CO)_4$, (c) $Fe^{II}(S_2C_2H_4)(CO)_2(dppv)$, (d) $Fe^{II}(S_2C_2H_4)(CO)_2(PMe_3)_2$, (e) $Na^+(THF)_2$:$[PhBP_3]Fe^{II}{\equiv}N(p\text{-tolyl})^-$, (f) $[PhBP_3]Fe^{III}{\equiv}N(p\text{-tolyl})$, (g) $[PhBP^{tBu}_3(pz')]Fe^{IV}{\equiv}N(t\text{Bu})^+$.

2.2. XAS measurements

X-ray absorption spectra were measured at the undulator beamline 4.0.2 at the Advanced Light Source (ALS) using a variable included angle grating monochromator as detailed elsewhere [29,30]. Samples were mounted on a liquid helium cooled cryostat cold finger in a UHV vacuum chamber. Fe L-edges were recorded by detection of the emitted photoelectrons concomitant with absorption using a channeltron electron multiplier. N K-edge absorption spectra were recorded in fluorescence yield mode. The fluorescence was detected using a 9 or 36-element superconducting tunnel junction (STJ) detector array [31]. A complete fluorescence spectrum was collected for each detector element and for each data point, allowing optimization of the fluorescence energy windows after data collection. Spectra were normalized to the incident radiation intensity measured either by using the photocurrent from a gold mesh or, optionally in the case of N K-edge fluorescence measurements, the integrated intensity of the carbon fluorescence peak. Energy calibration measurements were performed using appropriate standards immediately before and after each set of measurements. Fe L-edge measurements used either the lowest energy L_3 peaks of Fe_2O_3 at 708.0 eV or $K_3Fe(CN)_6$ at 706.8 eV. N K-edge measurements used either the pre-edge peak of boron nitride at 401.5 eV or the first pre-peak of $K_3Fe^{III}(CN)_6$ at 399.85 eV. Fe L-edge electron yield measurements were collected with the samples at room temperature. The N K-edge fluorescence-detected data were collected with sample temperatures down to 130 K, using temperatures below this limit caused interference from frozen N_2. For the electron-yield data, appropriate corrections usually had to be made to the first and second scan to correct for charging effects. By contrast, the high discrimination of STJ detector meant that fluorescence-detected data required no baseline correction.

3. Results

3.1. Survey

Before considering results for specific oxidation states in detail, we compare the starting point spectra for Fe(0) through Fe(IV) complexes in Fig. 1. For this paper we restrict ourselves to qualitative assignments of these spectra sufficient to provide initial interpretations of the observed

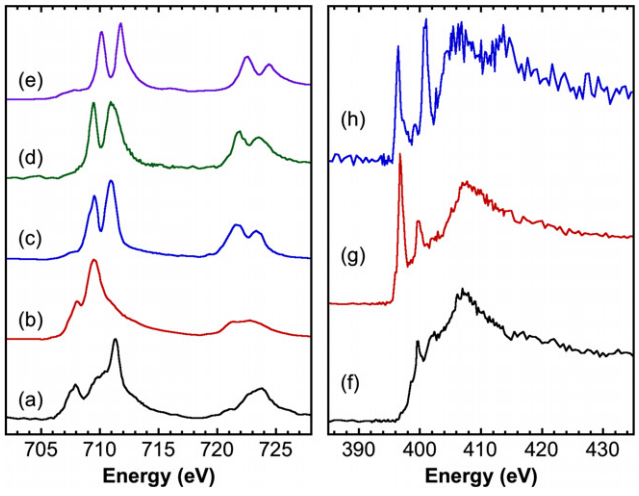

Fig. 1. Survey of soft X-ray spectra examined in this paper: (Left) Fe L_{23}-edges measured using electron-yield for (a) $(NEt_4)_2Fe^0(CO)_3(CN)_2$, (b) $Fe^I(pdt)(PMe_3)(CN)(CO)_4$, (c) $Fe^{II}(S_2C_2H_4)(CO)_2(PMe_3)_2$, (d) $Fe^{II}(S_2C_2H_4)(CO)_2(dppv)$, (e) $K_4Fe^{II}(CN)_6$ (Right) N K-edges measured using fluorescence detection for (f) $Na^+(THF)_2$:$[PhBP_3]Fe^{II}{\equiv}N(p\text{-tolyl})^-$, (g) $[PhBP_3]Fe^{III}{\equiv}N(p\text{-tolyl})$, (h) $[PhBP^{tBu}_3(pz')]Fe^{IV}{\equiv}N(t\text{Bu})^+$.

radiation chemistry. Detailed analyses of these data will be presented elsewhere.

Two distinct series of compounds were used. The first were Fe carbonyl complexes with cyanide, thiolate or trimethylphosphine ligands (Scheme 1). As expected for carbonyl compounds, they involve lower oxidation states, namely Fe(0), Fe(I) and Fe(II). These were studied using Fe $L_{2,3}$-edge spectroscopy, producing spectra with L_3 edges at approximately 710 eV and L_2 edges just above 720 eV (Fig. 1). The splittings apparent on both the L_3 and L_2 edges can be interpreted in both terms of the 3d ligand field splitting with $2p \rightarrow t_{2g}$ and $2p \rightarrow e_g$ transitions as well as the presence of $2p \rightarrow \pi^*$ metal–ligand charge transfer transitions [32]. The second series of compounds were mononuclear Fe imides, and these provided the higher oxidation states of Fe(II), Fe(III) and Fe(IV) (Scheme 1). These were studied by N K-edge spectroscopy (Fig. 1). The spectra are dominated by a broad K-edge at about 400 eV, preceded by sharp pre-edge features which involve nitrogen $1s \rightarrow 2p$ transitions into σ or π states, possibly with significant Fe 3d character. The pre-edge peak intensity is thus an indicator of the amount of N 2p character in a particular unoccupied molecular orbital.

3.2. Fe(0) L-edge spectra

Time-dependent L_3-edge spectra for a sample that was initially the Fe(0) complex $(NEt_4)_2Fe^0(CO)_3(CN)_2$ are shown in Fig. 2. Initially, the spectrum has two clear peaks at 707.8 and 711.3 eV. The first peak can qualitatively be assigned as a $2p \rightarrow e_g$ transition, while the latter can be assigned as a $2p \rightarrow \pi^*$ transition that gains intensity *via* dπ–pπ backbonding with the CO and CN^- ligands [32]. In subsequent scans, the strength of the band at 707.8 eV dramatically increases, and a shoulder at 710.3 eV becomes a stronger, resolved peak.

Two types of radiation chemistry need to be considered for these types of complexes: photooxidation of the Fe site and photolytic loss of CO ligands. For this low-spin d^8 complex, the simplest explanation is that the rise in intensity at 707.8 eV reflects an increase in the number of vacancies in the lowest energy orbitals. In very approximate terms, the complex is initially being oxidized from $t_{2g}^6e_g^2 \rightarrow t_{2g}^6e_g^1$ configuration, going from 2 to 3 holes in the e_g subshell. With additional exposure, the approximate doubling of the $2p \rightarrow e_g$ intensity suggests that oxidation may continue to Fe(II), thus going from 2 to 4 e_g vacancies. Of course, with the current measurement we cannot rule out direct 2-electron Fe(0) → Fe(II) oxidation as well.

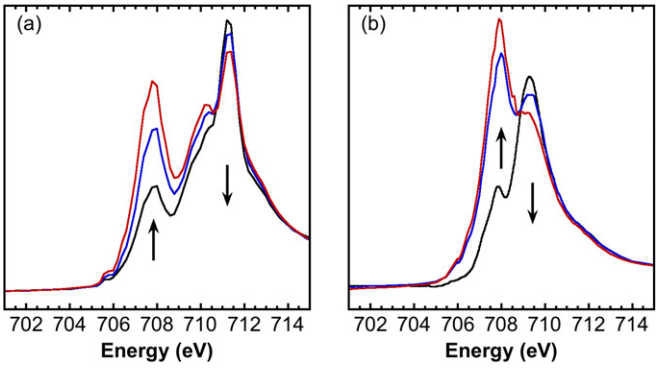

Fig. 2. Soft X-ray Fe L_3-edge spectra showing photochemistry of the Fe(0) and Fe(I) complexes. Arrows indicate direction of change with time. (a) $(NEt_4)2Fe^0(CO)_3(CN)_2$. The time of X-ray exposure at 708 eV for each scan was approximately 1 min, 5.5 min and 10 min. (b) $Fe^I(pdt)(PMe_3)(CN)(CO)_4$. The time of X-ray exposure at 708 eV for each sequential scan was approximately 2 min, 10 min and 18 min.

The time-dependent data in Fig. 2 allow an estimation of the approximate X-ray exposure needed to photolyze the sample by 50%, expressed either as the total energy deposited in the sample in Grays ($J\,kg^{-1}$) or the photon flux over a given surface area in photons/mm^2. For this calculation we only need an estimate of the time of exposure, the irradiated volume (image size × attenuation length), the sample density and the beamline flux (~1×10^{12} photons/s with 20 μm entrance and exit slits [29,30]). For this Fe(0) compound we found a 50% photolysis time of ~33 min, which corresponds to a dose of $2. \times 10^9$ Grays and 8.3×10^{16} photons/mm^2.

3.3. Fe(I) L-edge spectra

The data for the Fe(I) complex, $Fe_2^I(pdt)(PMe_3)(CN)(CO)_4$, are also shown in Fig. 2. Over time, there is again an increase in intensity in the low-energy region, and a band at 708.0 eV that was originally a low-energy shoulder eventually becomes the strongest peak in the spectrum. As there are two chemically distinct Fe(I) sites in the starting complex, there may be preferential photooxidation in the beam, and all we can say at this point is that the increase in the low-energy peak is consistent with oxidation of Fe(I) to Fe(II). We also note parenthetically that there is significantly less intensity in the 710–712 eV region compared to the previous spectrum for $(NEt_4)_2Fe^0(CO)_3(CN)_2$. This is consistent with less dπ–pπ backbonding because of the inclusion of phosphine and thiolate ligation in the $Fe_2^I(pdt)(PMe_3)(CN)(CO)_4$ complex. In any case, for this Fe(I) compound we estimate a 50% photolysis time of ~63 min which gives a radiation exposure of 3.2×10^9 Grays, and 1.1×10^{17} photons/mm^2.

3.4. Fe(II) L-edge spectra

Spectra for $Fe^{II}(S_2C_2H_4)(CO)_2(PMe_3)_2$ and $Fe^{II}2C_2H_4)(CO)_2$(dppv) as well as for $K_4Fe^{II}(CN)_6$ and $K_3Fe^{III}(CN)_6$ reference compounds, are shown in Fig. 3. The carbonyl complexes are relevant as models for the electronic state of Fe in the mononuclear hydrogenase known as 'Hmd Hydrogenase' [33]. Structurally they are very similar octahedral complexes except that in the complex coordinated by PMe_3 the carbonyl groups are both *trans* to thiolate, whereas for the complex containing the bidentate dppv ligand only one carbonyl is *trans* to thiolate whereas the

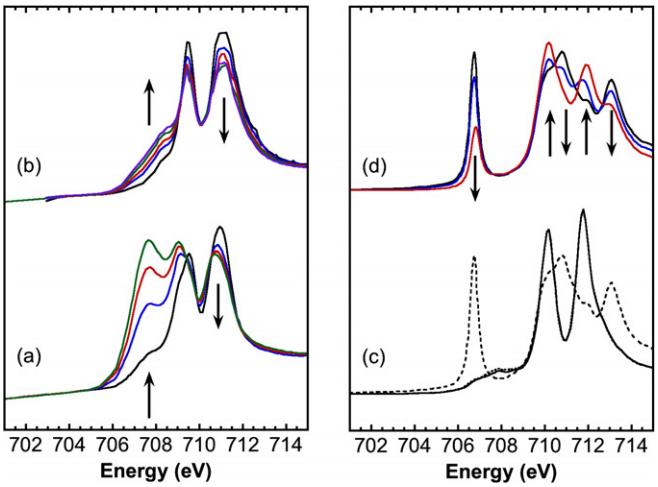

Fig. 3. (Left) X-ray photochemistry observed by Fe L_3-edge spectroscopy for (a) $Fe^{II}(S_2C_2H_4)(CO)_2(PMe_3)_2$ and (b) $Fe^{II}(S_2C_2H_4)(CO)_2$(dppv). Arrows indicate direction of change for sequential scans. In both cases each scan took about 7 min. The measured beam intensity for (b) was 3-fold greater than for (a). (Right) (c) A comparison of spectra for $K_4Fe^{II}(CN)_6$ (solid) and K_3Fe^{III} $(CN)_6$ (broken). Note that the $K_4Fe^{II}(CN)_6$ plot is a superimposition two spectra taken 1 h apart. (d) X-ray photoreduction of $K_3Fe^{III}(CN)_6$ to the Fe^{II} form.

other is *trans* to the phosphino ligand. Since their ligands are so similar, it is not surprising that the spectra for $Fe^{II}(S_2C_2H_4)(CO)_2(PMe_3)_2$ and $Fe^{II}(S_2C_2H_4)(CO)_2$(dppv) are very similar, each with a pair of strong peaks at 709.5 eV and 710.9 eV, similar to the spectrum for $K_4Fe^{II}(CN)_6$. These are both octahedral low-spin Fe(II) complexes with filled t_{2g} orbitals, therefore the twin peaks are neither a ligand field splitting nor a multiplet effect. Instead, they result from p-backbonding with the CO or CN^- ligands, resulting in allowed character for $2p \rightarrow p^*$ transitions [32], and the observed splitting is between e_g and p^* levels.

Despite the initially similar spectra, the X-ray photochemistries of $Fe^{II}(S_2C_2H_4)(CO)_2(PMe_3)_2$ and $Fe^{II}(S_2C_2H_4)(CO)_2$(dppv) are significantly different. During scans of the L_3 region, changes are seen in the spectra from both complexes. For $Fe^{II}(S_2C_2H_4)(CO)_2(PMe_3)_2$ the changes are rapid, with some effects likely before the first scan is even completed. A band at 707.6 eV grows stronger with each sweep (Fig. 3) and soon dominates the spectrum. Additional more subtle changes are also seen, including a downshift to 709.0 eV and increased intensity for the peak at 709.5 eV, as well as a loss in intensity and decrease in energy for the other main feature initially at 710.9 eV. By contrast, for $Fe^{II}(S_2C_2H_4)(CO)_2$(dppv) the changes are much slower and it was necessary to increase the X-ray intensity about 3-fold to get a reasonable rate. At this X-ray intensity, similar changes with time are seen in the bands at 709.5 eV and 710.9 eV in compared with the PMe_3 coordinated complex. However, the rate of increase broad band seen growing between 706 eV and 707 eV is substantially slower and achieves only about 20% of the intensity of the corresponding feature in PMe_3 complex (Fig. 3). This is reflected in the estimated radiation exposure for 50% photolysis. Using the peak changes at ~709 eV, we estimate exposure times of 10 min and 83 min for the PMe_3 and dppv complexes respectively, which, after allowing for the difference in X-ray flux, gives a radiation exposure of 1.7×10^8 Grays and 5.6×10^{15} photons/mm^2 for the PMe_3 complex as well as 4.2×10^9 Grays and 1.4×10^{17} photons/mm^2 for the compound containing the bidentate dppv ligand.

It is instructive to contrast these changes with the differences between $K_4Fe^{II}(CN)_6$ and $K_3Fe^{III}(CN)_6$. The Fe(II) hexacyanide also gives a L_3-edge spectrum containing two bands this time at 710 eV and 711.8 eV. On oxidation to Fe(III), a sharp low-energy band appears at 706.8 eV. In addition, the relative intensity of the two higher energy peaks is reversed, accompanied by an increase in energy of approximately 1 eV (Fig. 3). As for X-ray photochemistry, the $L_{2,3}$-edge spectrum of the Fe(II) complex shows very little change after 2 h of soft X-ray scanning at these energies and X-ray intensities (Fig. 3). By contrast, the Fe(III) complex cleanly photoreduces to the Fe(II) form (Fig. 3) with four clear isosbestic points.

This allows a straightforward assignment for the changes in the carbonyl spectra – the new low-energy feature at ~707 eV arises from a $2p \rightarrow 3d$ ("t_{2g}") transition on the photolyzed Fe site. The simplest interpretation is that the Fe(II) complex is being photooxidized to a low-spin Fe(III) complex. However, the differences seen in the radiation dependent spectra of the two carbonyl complexes indicate additional chemistry might be occurring in these complexes. Some of the intensity changes may arise from X-ray photolysis, most likely of a carbonyl ligand. It could well be that the changes in Fig. 3 are a combination of photooxidation and photolysis. In any case, the observed dependence of the X-ray photochemistry on the coordination stereochemistry is intriguing and offers the prospect that these measurements may assist in the structural assignment from L-edge spectra.

3.5. Fe(III) nitrogen K-edge spectra

The second series of complexes involves iron imides in Fe(II), Fe(III), and Fe(IV) oxidation states. For these complexes, we found that observation from the ligand point of view, in this case using the nitrogen K-edge, provided simple and directly interpretable spectra. We begin with time-dependent nitrogen K-edge data for $[PhBP_3]Fe^{III}{\equiv}N$ (*p*-tolyl), which are shown in Fig. 4. The Fe(III) spectrum is characterized by two sharp features at 396.8 eV and 399.8 eV, followed by a broad peak centered at 407.5 eV. In contrast, reduction to the Fe(II) form apparently removes the 396.8 eV peak, but does not substantially change the band at 399.8 eV and the broad band at 407.5 eV (Fig. 4).

The exact nature of the transitions in this aryl-imide requires more thorough study such as a full density functional theory (DFT) analysis, however, one possible

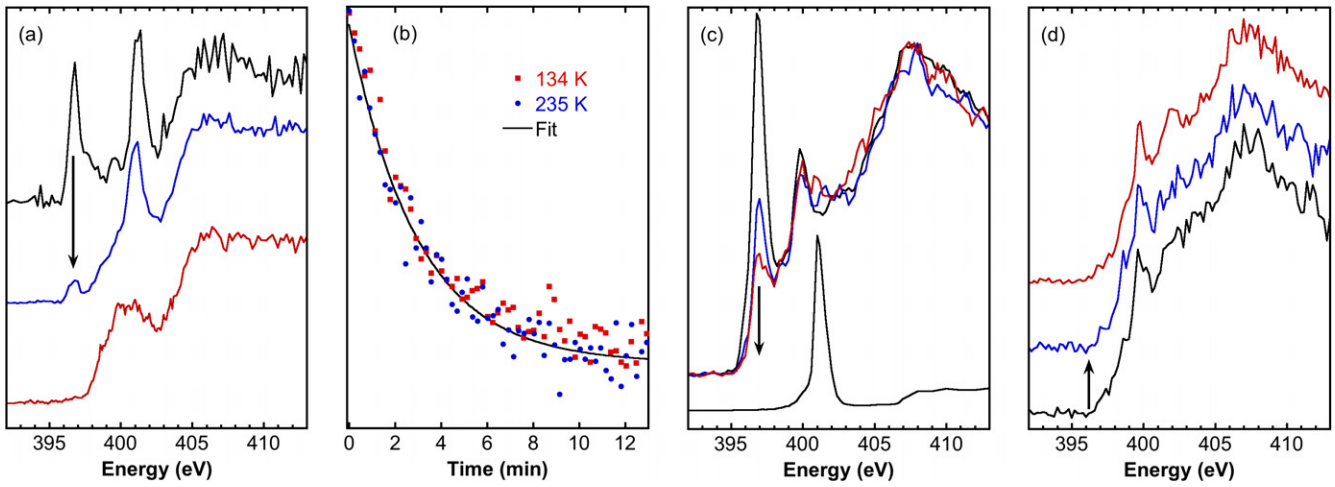

Fig. 4. X-ray photochemistry observed using N K-edge spectroscopy on Fe imide complexes. Arrows indicate direction of change for sequential scans. (a) Photochemistry of $[PhBP_3^{tBu}(pz')]Fe^{IV}{\equiv}N(tBu)^+$. (b) Time-course observed at 396.7 eV for $[PhBP_3^{tBu}(pz')]Fe^{IV}{\equiv}N(tBu)^+$ measured at 134 K and 235 K. The fit is a simple exponential decay with a time constant of 3.0 min. (c) (top) Photoreduction of $[PhBP_3]Fe^{III}{\equiv}N(p\text{-tolyl})$ to the Fe(II) form. (bottom) Solid frozen N_2 measured at ~30 K (d) Successive scans on $[Na^+(THF)_2{:}[PhBP_3]Fe^{II}{\equiv}N(p\text{-tolyl})^-$ showing the lack of photochemistry.

explanation centers on the "octahedral-like" splitting suggested by DFT analysis on the equivalent alkyl-imide [27]. The observed single pre-edge band in the Fe(II) spectrum can then be explained in terms of a transition to the two unoccupied upper levels and the intensity of the transition reflects the N 2p contribution to the molecular orbital. In this model, for the higher oxidation states, additional transitions are possible to the partially occupied lower 3d orbitals coupled to N $2p\sigma^*$ giving rise to additional lower energy bands.

Examination of Fig. 4 reveals that the $Fe(III)[PhBP_3]$-$Fe{\equiv}N(p\text{-tolyl})$ complex undergoes a straightforward photoreduction to the Fe(II) form. Although this spectrum was measured at 135 K, essentially identical results were obtained at room temperature. The sharp feature at 396.8 eV gradually disappears, while that at 399.8 eV is essentially unchanged. For this process, we estimate a 50% photolysis time of ~28 min, which gives a radiation exposure of 3.0×10^9 Grays, and 4.5×10^{16} photons/mm^2. By contrast, the Fe(II) complex is unaffected by irradiation (Fig. 4), at least on the hour-long timescale of these experiments.

3.6. Fe(IV) nitrogen K-edge spectra

The photochemistry for the sole Fe(IV) compound in this study, $[PhBP_3^{tBu}(pz')]Fe^{IV}{\equiv}N(tBu)^+$, shows two distinct phases, with an apparently well-defined intermediate step. The nitrogen K-edge of the starting complex comprises two relatively intense sharp bands at 396.7 eV and 401.2 eV, with weak shoulder apparent at 397.8 eV as well as the usual broad band at around 407 eV (Fig. 4). After about 5 min of X-ray irradiation the spectrum completely changes. The intense peak at 396.7 eV is replaced by a much weaker structure centered at 396.6 eV while the band at 401.2 eV downshifts to 401.0 eV. In addition there is evidence of an underlying broad feature growing centered at ~400 eV (Fig. 4). As fluorescence measurements do not suffer from the time-dependent charging phenomena that make electron-yield time-courses difficult to collect, we were able to measure the time-course of this reaction at both 134 K and 235 K and these data are presented in Fig. 4. It is apparently independent of temperature and shows an apparent simple exponential decay which probably arises in part from thickness effects. After an additional 30 min irradiation the spectrum has changed again, there is now no obvious sign of the two sharp peaks and the pre-edge is now dominated by the broad feature at ~400 eV (Fig. 4).

The simplest interpretation of this chemistry is that the first rapid stage is a clean photoreduction to a well-defined Fe(III) form. Of course, without further analysis we cannot rule out a 2-electron reduction to Fe(II). For this process, we estimate a 50% photolysis time of 2 min, which gives a radiation exposure of 4.1×10^8 Grays and 8.3×10^{15} photons/mm^2. This is then followed by the second stage. As the reduced states of the Fe imide are all expected to exhibit sharp peaks in the N K-edge spectrum, we assign this process to a photocatalyzed structural change of the cluster.

4. Discussion

This paper explores whether measurements of soft X-ray photochemistry can be a chemically useful spectroscopic tool, in particular for characterizing biological metal centers. Our motivation is related to the mission of the Advanced Biological and Environmental X-ray facility (ABEX) based at the ALS, which is to develop soft X-ray spectroscopy as tool to probe metal sites in both biological systems and the environment. A significant fraction of our work involves measurements on metalloproteins [34]

and quantitating and consequently minimizing X-ray photochemical change has become a routine part of our measurements. Very often, we observe apparently well-defined spectroscopic changes on radiation exposure. Iron–sulfur clusters, for example exhibit broad Fe $L_{2,3}$-edge envelopes that gradually shift to lower energy as the clusters are photoreduced. Another example is the Fe $L_{2,3}$-edge of Hmd hydrogenase, which comprises a structured spectrum that undergoes an apparently well-defined photochemical change with isosbestic points. Since the collection of photochemical data on these samples is a routine by-product of soft X-ray measurements, the proposition that it can be interpreted to yield chemically useful information is very attractive.

Not surprisingly, the photochemical changes seen by soft X-ray spectroscopy in the series of Fe compounds examined in this paper apparently depend on the Fe oxidation state. The Fe(IV) and Fe(III) complexes were rapidly photoreduced in the X-ray beam, while conversely, Fe(I) and Fe(0) complexes show strong evidence of photooxidation. The Fe(II) complexes showed either no observed photochemistry, or a tendency to be photooxidized. Several of the complexes showed evidence of more than one chemical process. The carbonyl complexes, in particular the Fe(II) compounds, showed evidence of photooxidation and ligand photolysis, while the Fe(IV) imide showed a clear biphasic reaction, with a well-defined photoreduction being followed by a less well-defined photochemical structural change.

We now compare the radiation doses required to cause photochemical change, for a variety of samples and techniques. Table 1 summarizes the radiation exposure estimates for biological samples, including (hard) X-ray crystallography on protein crystals [5,17,37] and soft X-ray microscopy on living cells [36], as well as the range of required doses that we have observed for Fe compounds in this work. Comparison of these data shows some well-known and not unexpected trends. First, the most fragile material is living yeast, which shows 50% mortality after a 4×10^4 Gy dose of soft X-rays. Protein crystals are more robust, with 50% loss of diffraction occurring around the well-known Henderson Limit of 2×10^7 Gy [17], although recent studies indicate that this may be a slight underestimate [35]. The metal centers within protein crystals can sometimes be significantly more susceptible to damage, as shown by the data on photosystem II [4] and superoxide reductase [5] which have radiation dose limits in the 10^5–10^6 Gy range. (These metal centers are particularly sensitive to X-ray irradiation, and other sites may require a much larger exposure.) In any case, it is worth emphasizing that the estimated metalloprotein X-ray dose limits ($\sim 10^{14}$–10^{15} photon/mm^2) are readily achieved within minutes (or even seconds) on modern focused hard X-ray beamlines.

Table 1 shows that the Fe compounds presented here are all significantly more tolerant to X-ray photochemical change than the biological systems. Most of the complexes require about 2×10^9 Gy for a 50% effect, the more sensitive Fe(IV) imide complex requires about an order of magnitude less, while compounds such as potassium ferrocyanide are significantly more robust. Taken at face value, one might conclude that metal centers more are resistant to photoreduction than protein crystals are to loss of diffraction. However there are concentration and temperature effects to consider. It is likely that these radiation dose estimates will not depend on concentration if the photochemistry is oxidative or involves ligand dissociation as these processes probably involve direct X-ray absorption by the chemically active group. Photoreduction, however, arises from liberated electrons from the surrounding matrix, and so, more dilute materials could well see a greater sensitivity as the number of available electrons is proportionately greater. On the other hand it is well known that low temperatures reduce the rate of radiation photoreduction, presumably, because electrons and electron holes become trapped in amido and other sites (for example [38] and references therein). A quantitative study comparing the stability of metal centers in frozen solutions, proteins, solids, protein crystals would clearly be of interest.

A key question is whether X-ray radiation-induced spectroscopic changes are sufficiently well defined to help diagnose chemical information about the center under study. Certainly, in the cases presented here, all the compounds

Table 1
A survey of estimated radiation dose levels required to induce photochemical effects

Sample	Technique (energy)	Photochemical radiation dose limit			Ref.
		Criterion	(Grays)	(photons/mm^2)	
Protein crystal (Henderson limit)	X-ray diffraction (8 keV) (calculated from electron diffraction)	50% loss of diffraction	2×10^7	1.6×10^{16}	[17]
Holoferritin crystal	X-ray crystallography (13 eV)	50% loss of diffraction	3×10^7	2×10^{16}	[35]
Photosystem II crystal	X-ray crystallography (13.3 keV)	50% change in metal cluster	2.2×10^6	5×10^{15}	[4]
Superoxide reductase crystal (Fe(III) center)	X-ray crystallography (13.5 keV)	25% change in metal site	2.7×10^5	1.5×10^{14}	[5]
Yeast cells and myofibrils	X-ray microscopy (400 eV)	50% yeast survival	4×10^4	3×10^{11}	[36]
Fe complexes	soft XAS (380–750 eV)	50% change in spectrum	2×10^8–4×10^9	5.6×10^{15}–1.4×10^{17}	this work

have significantly different photochemical behavior. The Fe(IV) imide, for instance, has a clear biphasic X-ray photochemistry, with an rapid initial photoreduction followed by a well-defined, although currently chemically unclear, second step. By contrast, the Fe(III) imide exhibits only a single relatively slow photoreduction to the Fe(II) form. The most interesting case, however, is the comparison of the Fe(II) complexes. The Fe L_3-edge spectra for three of the compounds presented here, $Fe^{II}(S_2C_2H_4)(CO)_2(PMe_3)_2$, $Fe^{II}(S_2C_2H_4)(CO)_2$(dppv) and $K_4Fe^{II}(CN)_6$ (Fig. 1) are very similar, each having a pair of strong peaks centered at about 710 eV. The X-ray induced photochemistry of the three complexes, however, is very different as illustrated by both the spectra in Fig. 3 and the dose limit estimates in Table 1. The hexacyanide shows very little observed changes with the X-ray dose level investigated in this paper. By contrast, the complex ligated by dppv and carbonyl, which has one CO *cis* to thiolate and one CO *trans* to the thiolate ligand, shows relatively slow changes that seem photooxidative in nature. However, the Fe(II) carbonyl complex coordinated by PMe_3 which has analogous ligands to the dppv complex but with different stereochemistry in that both CO groups are *cis* to thiolate, shows a much more rapid, spectroscopically distinct X-ray photochemistry, as indicated by the significant change at 707.6 eV compared to the Fe(II). Clearly, a proper understanding of such X-ray photochemical effects would greatly assist the understanding and possibly even the structural assignment of an uncharacterized metal site in, for example, a metalloprotein. Therefore, we conclude that soft X-ray monitored X-ray photochemistry could well comprise a useful addition to the spectroscopist's repertoire.

Finally, if time-dependent measurement is to become a useful part of the soft X-ray spectroscopists tool chest, it is worth commenting on the technical issues underlying these measurements with existing beamlines. If fluorescence detection is used, then single energy measurements measurement of these kinetic effects is straightforward, at least with a second data point interval, as the measurement in Fig. 4 shows. Electron-yield measurements, using for example a channeltron to quantitate the photoelectrons, are more problematic as, when the X-ray beam is first applied to the sample, an often irreproducible time-dependent decay arising from charging or capacitance effects can dominate the spectrum for several minutes. The obvious solution of alternating the monochromator rapidly between two more energies over a timescale of a few seconds requires the beamline to be designed to be both capable of such rapid scanning and reliable enough to remain accurately within energy calibration as the energy is alternated. At this time, such beamlines are not commonly available.

A closely related issue is how best to measure the soft X-ray spectrum of a photosensitive sample. With a modern high brightness beamline such as ALS beamline 4.0.2, many samples, such as those presented in this paper, show X-ray photochemical changes over the typical scan time of 20 min. Importantly, these comprise not just biological samples such as metalloproteins, but will almost certainly include any catalytic material with a redox active metal center. Often, in order to measure a "damage free" spectrum, it is necessary to significantly reduce the flux of the beamline. Again, a rapid scanning beamline would enable the measurement of a such a spectrum on the timescale of a minute or less on full flux. Averaging several scans, with each using a fresh sample spot, could then enhance the statistics of the spectrum. Such facilities would enable the soft X-ray spectroscopist interested in to properly take advantage of today's high brightness synchrotron light sources, collecting good spectra in much shorter times as well as exploiting the potential of soft X-ray photochemistry.

5. Conclusion

We have examined the time-dependent soft X-ray absorption spectra for a series of Fe complexes with formal oxidation states from Fe(IV) to Fe(0). Often, well-defined chemistry occurs, which is capable of straightforward interpretation in terms of X-ray induced photoreduction or oxidation, and in some cases ligand photolysis. We have demonstrated that the X-ray photochemistry not only depends on the Fe oxidation state but also the coordination chemistry of the complex.

Software engineers often joke that "it's not a bug, it's a feature". In a similar spirit, we note that radiation 'damage' has often been derided as a problem inherent to X-ray spectroscopy that needs to be overcome. It now seems that a proper understanding of such X-ray photochemical effects could greatly assist the assignment of soft X-ray spectra of uncharacterized metal sites. In this way the "bug" of radiation photochemistry could well become an important feature of the technique.

Acknowledgements

One of us (S.P.C.) would especially like to thank Ed Solomon for hosting him during 'mini-sabbaticals' at Stanford. The group meetings were always intellectually stimulating, and the frequent birthday cakes were a special treat.

We thank the ALS staff, in particular Drs. Elke Arenholtz and Anthony Young for their support of beamline 4.0.2. This work was funded by NIH Grant EB-001962 (SPC). ABEX is supported by the DOE Office of Biological and Environmental Research. J.C.P. gratefully acknowledges support from the NSF (CHE-0132216), the DOE (PECASE), and the Alfred P. Sloan Foundation. T.B.R. thanks the NIH (GM-061153) for support. The Advanced Light Source is supported by the DOE Office of Science, Office of Basic Energy Sciences.

Appendix A. Supplementary material

Supplementary data associated with this article can be found, in the online version, at doi:10.1016/j.ica.2007.10.039.

References

[1] L. Powers, W.E. Blumberg, B. Chance, C.H. Barlow, J.S. Leigh Jr., J. Smith, T. Yonetani, S. Vik, J. Pelsach, Biochim. Biophys. Acta 546 (1979) 520.
[2] G.W. Brudvig, D.F. Bocian, R.C. Gamble, S.I. Chan, Biochim. Biophys. Acta 624 (1980) 78.
[3] B. Chance, P. Angiolillo, E.K. Yang, L. Powers, FEBS Lett. 112 (1980) 178.
[4] J. Yano, J. Kern, K.-D. Irrgang, M.J. Latimer, U. Bergmann, P. Glatzel, Y. Pushkar, J. Biesiadka, B. Loll, K. Sauer, J. Messinger, A. Zouni, V.K. Yachandra, Proc. Natl. Acad. Sci. USA 102 (2005) 12047.
[5] V. Adam, A. Royant, V. Nivière, F.P. Molina-Heredia, Structure 12 (2004) 1729.
[6] A. Karlsson, J.V. Parales, R.E. Parales, D.T. Gibson, H. Eklund, S.J. Ramaswamy, Inorg. Biochem. 78 (2000) 83.
[7] D.T. Logan, X.-S. Su, A. Åberg, K. Regnström, J. Hajdu, H. Eklund, P. Nordlund, Structure 4 (1996) 1053.
[8] T. Beitlich, K. Kuhnel, C. Schulze-Briese, R.L. Shoeman, I.J. Schlichting, Syn. Rad. 14 (2007) 11.
[9] S.J. Yoo, H.C. Angove, V. Papaefthymiou, B.K. Burgess, E. Münck, J. Am. Chem. Soc. 122 (2000) 4926.
[10] F. Champloy, K. Gruber, G. Jogl, C.J. Kratky, Syn. Rad. 7 (2000) 267.
[11] J. Wuerges, J.-W. Lee, Y.-I. Yim, H.-S. Yim, S.-O. Kang, K.D. Carugo, Proc. Natl. Acad. Sci. USA 101 (2004) 8569.
[12] O. Carugo, K.D. Carugo, TIBS 30 (2005) 213.
[13] J. Peisach, L. Powers, W.E. Blumberg, B. Chance, Biophys J. 38 (1982) 277.
[14] J.E. Penner-Hahn, M. Murata, K. Hodgson, H.C. Freeman, Inorg. Chem. 28 (1989) 1826.
[15] M.E. Stroppolo, S. Nuzzo, A. Pesce, C. Rosano, A. Battistoni, M. Bolognesi, S. Mobilio, A. Desideri, Biochem. Biophys. Res. Commun. 249 (1998) 579.
[16] W.A. Hendrickson, J, Mol. Biol. 106 (1974) 889.
[17] R. Henderson, Proc. Roy. Soc. Lond. B 241 (1990) 6.
[18] J. Maser, A. Osanna, Y. Wang, C. Jacobsen, J. Kirz, S. Spector, B. Winn, D.J. Tennant, Microscopy 197 (2000) 68.
[19] W.H.J. Massover, Syn. Rad. 14 (2007) 116.
[20] E.F. Garman, S.M.J. McSweeney, Syn. Rad. 14 (2007) 1.
[21] D. Sayre, J. Kirz, R. Feder, D.M. Kim, E. Spiller, Science 196 (1977) 1339.
[22] M.O. Krause, J. Chem. Phys. Ref. Data 8 (1979) 307.
[23] M. Schiltz, G.J. Bricogne, Syn. Rad. 14 (2007) 34.
[24] F. Gloaguen, J.D. Lawrence, M. Schmidt, S.R. Wilson, T.B. Rauchfuss, J. Am. Chem. Soc. 123 (2001) 12518.
[25] A. Kayal, T.B. Rauchfuss, Inorg. Chem. 42 (2003) 5046.
[26] C.M. Thomas, N.P. Mankad, J.C. Peters, J. Am. Chem. Soc. 128 (2006) 4956.
[27] S.D. Brown, J.C. Peters, J. Am. Chem. Soc. 127 (2005) 1913.
[28] C.Y. Ralston, H. Wang, S.W. Ragsdale, M. Kumar, N.J. Spangler, P.W. Ludden, W. Gu, R.M. Jones, D.S. Patil, S.P. Cramer, J. Am. Chem. Soc. 122 (2000) 10553.
[29] A.T. Young, J. Feng, E. Arenholz, H.A. Padmore, T. Henderson, S. Marks, E. Hoyer, R. Schlueter, J.B. Kortright, V. Martynov, C. Steier, G. Portmann, Nucl. Instrum. Meth. A 467 (2001) 549.
[30] A.T. Young, E. Arenholz, J. Feng, H. Padmore, S. Marks, R. Schlueter, E. Hoyer, N. Kelez, C. Steier, Surf. Rev. Lett. 9 (2002) 549.
[31] S. Friedrich, T. Funk, O. Drury, S.E. Labov, S.P. Cramer, Rev. Sci. Instrum. 73 (2002) 1629.
[32] R.K. Hocking, E.C. Wasinger, F.M.F. de Groot, K.O. Hodgson, B. Hedman, E.I. Solomon, J. Am. Chem. Soc. 128 (2006) 10442.
[33] S. Shima, S.K. Thauer, Chem. Record 7 (2007) 37.
[34] T. Funk, A. Deb, S.J. George, H. Wang, S.P. Cramer, Coord. Chem. Rev. 249 (2005) 3.
[35] R.L. Owen, E. Rudino-Pinera, E.F. Garman, Proc. Natl. Acad. Sci. USA 103 (2006) 4912.
[36] H. Fujisaki, S. Takahashi, H. Ohzeki, K. Sugisaki, H. Kondo, H. Nagata, H. Kato, S. Ishiwata, J. Microsc.- Oxford 182 (1996) 79.
[37] M.L. Ghirardi, P.W. King, M.C. Posewitz, P.C. Maness, A. Fedorov, K. Kim, J. Cohen, K. Schulten, M. Seibert, Biochem. Soc. Trans. 33 (2005) 70.
[38] M.C.R. Symons, Free Rad. Biol. Med. 22 (1996) 1271.